

Design and Optimization of a Gripper Clamp

M. S. Cunha

Department of Metallurgical and Materials Engineering, Faculdade de Engenharia, Universidade do Porto, Rua Dr. Roberto Frias, 4200-465 PORTO, Portugal (up201806584@edu.fe.up.pt) ORCID [0000-0002-1608-6932](https://orcid.org/0000-0002-1608-6932)

E. S. Alves

Department of Metallurgical and Materials Engineering, Faculdade de Engenharia, Universidade do Porto, Rua Dr. Roberto Frias, 4200-465 PORTO, Portugal (up201806565@edu.fe.up.pt) ORCID [0009-0004-8677-0125](https://orcid.org/0009-0004-8677-0125)


J. M. Costa

Department of Metallurgical and Materials Engineering, Faculdade de Engenharia, Universidade do Porto and LAETA/INEGI - Institute of Science and Innovation in Mechanical and Industrial Engineering, Rua Dr. Roberto Frias, 4200-465 PORTO, Portugal (jose.costa@fe.up.pt) ORCID [0000-0002-1714-4671](https://orcid.org/0000-0002-1714-4671)


Author Keywords

Additive Manufacturing, Laser Powder Bed Fusion, AISI 316L Stainless Steel, Design for Additive Manufacturing, Topological Optimization Fusion 360, nTopology.

Type: Research Article

 Open Access

 Peer Reviewed

 CC BY

Abstract

Additive Manufacturing, among the many developing advanced manufacturing technologies, stands out as the one with the greatest potential for changing the distribution of manufacturing, society, and sustainability. To produce sustainable and competitive products, component material and design selection is an essential and critical topic in the industry. The production of parts designed using the Design for Additive Manufacturing methodology (DfAM) has grown in popularity in recent years. Topological optimization can be used as a design tool in the early stages of the design process to meet strength and endurance requirements on a component level. This study explores the topology optimization of a gripper clamp through nTopology and Fusion 360, using AISI 316L stainless steel as material, for production through Additive Manufacturing. The final component demonstrated reliable results.

1. Introduction

The progression of advanced manufacturing technology is ushering in notable transformations in the scale and dispersion of manufacturing processes. This shift is primarily driven by escalating consumer demands for highly customized goods and services, coupled with growing apprehensions regarding the ecological implications of global production systems (Ford and Despeisse 2016). Additive manufacturing (AM) is a manufacturing technology that aligns with these trends. Additive manufacturing (AM) is a constructive technology that has evolved significantly over the last three decades. Conceived initially as a groundbreaking and disruptive technology primarily intended for prototyping, it has since evolved to encompass the production of functional and structural components characterized by intricate geometries and custom-tailored structures that simultaneously exhibit reduced weight (DebRoy et al. 2018; Gorse et al. 2017). This evolution has enabled the significant personalization of manufactured components, making it particularly appealing to industries such as aerospace and biomedical. The methodology allows for producing near-net shape components with complex geometries at minimal additional cost (Costa et al. 2021; Bedmar et al. 2022).

In contrast to conventional subtractive and formative manufacturing methodologies, the American Society for Testing and Materials (ASTM) defines AM as a process of joining materials to make objects from 3D model data, usually layer upon layer (ISO/ASTM 2015). This process entails the deposition of raw material on a base that progressively shifts following the creation of each layer, maintaining a consistent distance between the base and the layer. A potentially complex geometrical component is obtained and removed from the base bed (Tofail et al. 2018).

Fused filament fabrication (FDM), Powder bed fusion (PBF), Stereolithography (SLA), Selective laser melting (SLM), Selective laser sintering (SLS), and digital light processing (DLP) are some of the most extensively utilized AM technologies (Ford and Despeisse 2016). However, to determine the best AM technology to use, it is crucial to evaluate and select the component design that will be manufactured, the required metallurgical (chemical composition and microstructure) as well as the mechanical properties (tensile strength, impacts), finishing (roughness, distortion, and shrinkage), costs, and supply chain conditions (Herderick 2011; Huang et al. 2015; Gibson, Rosen and Stucker 2010). On the other hand, an essential requirement for achieving an effective joining in AM, regardless of the technology used, is an effective combination of feedstock (or raw) material and good energy delivery. Within AM techniques, Laser powder bed fusion (LPBF) stands out. LPBF leverages a powdered feedstock, distributed as a bed layer, and selectively melted by a laser source to incrementally construct components layer by layer, all under the protection of an inert atmosphere, such as argon (King et al. 2015; Zitelli, Folgarait and Di 2019; Criales et al. 2017; Khairallah et al. 2016). LPBF is highly affected by numerous variables, which have a direct impact on the microstructure in the physical and mechanical properties of the components manufactured through this process, such as surface finish, elongation, strength, and hardness. These variables can be grouped into powder characteristics (chemical composition, powder morphology, and granulometry) and process parameters (Irrinki et al. 2020). Regarding the processing parameters that have the greatest influence on the quality of the components produced by LPBF, it is possible to highlight the laser power (P), the scan speed of the laser (v), the distance between consecutive laser scans, known as hatch spacing (h), and the powder layer (t). Properly managing and optimizing these parameters is of utmost importance in mitigating potential defects and stress-related issues such as porosity, anisotropy, residual and thermal stresses, keyholding, the balling effect, internal cracks, and alterations in chemical composition (Diaz Vallejo et al. 2021).

Design for Additive Manufacturing (DfAM) has recently piqued the design and engineering research community's interest. It can be understood as the process of creating, optimizing, or adapting the form and function of a part, assembly, or product to fully utilize the advantages of AM processes (Costa et al. 2021). Thus, respecting the methodologies of this technology and at the same time taking advantage of its unique capabilities, it is possible to achieve an interesting performance. A prominent strategy within the DfAM framework is Topological Optimization (TO). TO is a mathematical method for optimizing the spatial distribution of material within a defined domain by satisfying previously established constraints and minimizing a predefined cost function (Rosinha et al. 2015; Oliveira, Maia and Costa 2023). This technique relies on finite element analysis (FEA), where an algorithm is employed to determine the spatial configuration that best meets the prescribed performance criteria (Mata, Pinto and Costa 2023). The three main elements of such an optimization procedure are design variables, cost function, and constraints. This way, the primary goal is to achieve the desired functionality for a given set of loads and constraints while optimizing for

characteristics such as minimal material usage/weight or uniform stress distribution. Overall, TO enables mass reduction, stiffness optimization within the confines of a maximum allowed volume, and the calibration of load settings to attain specific volume reduction objectives (Costa et al. 2021).

This study, as its central focus, aimed to optimize a gripper clamp employing nTopology and Fusion 360 software. The intended outcome was to enable the potential production of this optimized design using the LPBF technique, utilizing AISI 316L stainless steel as the material of choice.

2. Materials and Methods

2.1. AISI 316L stainless steel

The material used for this study was AISI 316L stainless steel, where the typical powder composition is presented in Table 1.

Element	C	P	Si	Ni	Mn	S	Cr	Mo	Fe
Wt%	0.03	0.02	0.75	14.00	2.00	0.01	18.00	2.62	Bal.

Table 1: Typical composition of 316L metallic powders for LPBF, (Ronneberg, Davies, and Hooper 2020).

AISI 316L stainless steel manufactured through LPBF presents a complex as-built microstructure because of its high heating and cooling rates, induced thermal gradients, and non-equilibrium solidification. This specific stainless steel variant is characterized by its significant nickel content, along with substantial levels of chromium and molybdenum, rendering it prone to the formation of intermetallic phases such as Sigma (σ), Chi (χ), or Laves (η) phases or carbides such as $M_{23}C_6$ or M_6C after long term exposure to temperatures ranging from 550 to 900°C. It is worth emphasizing that the presence of the σ phase, in particular, should be diligently avoided, as it adversely affects ductility and fracture toughness (ASM 2004; Tang 2005). Specifically, the presence of chromium, greater than 16 wt.%, contributes to forming a stable passive oxide rich in chromium on the surface and confers excellent corrosion resistance. On the other hand, the 316L produced by LPBF also presents, in general, a superior corrosion resistance when compared to the one obtained by traditional technologies since MnS inclusions are not present. Furthermore, this alloy maintains a low carbon content of 0.03 wt.% and is renowned for its commendable weldability. In terms of weldability, mechanical properties, and corrosion resistance, AISI 316L is highly sought after in various applications, including marine, fuel cell technologies, and biomedical equipment. Table 2 provides an overview of the typical mechanical properties associated with this material (Vallejo et al. 2021).

Young's modulus	190-205 GPa
Specific Stiffness	23.8-25.8 MN.m/kg
Yield Strength (elastic limit)	170-310 MPa
Tensile Strength	485-560 MPa
Tensile Strength with Temperature	541-541 MPa
Elongation	30-50 %strain
Compressive strength	170-310 MPa
Hardness - Vickers	170-220 HV
Fracture toughness	53-72 MPa.m ^{0.5}

Table 2: Typical mechanical properties for 316L (Granta CES EDUPACK, 2022).

2.2. Topology Optimization

The initial phase in commencing this project involved the selection of a Computer-Aided Design (CAD) model. The chosen CAD model features specific dimensional attributes, namely

a mass of 5.21 kilograms, a height of 212 centimeters, a width of 15 centimeters, and a depth of 7 centimeters, as visually depicted in Figure 1. Regarding the three individual clamps, each clamp possesses distinct measurements, characterized by a height of 5.50 centimeters, a width of 1.40 centimeters, and a depth of 1.95 centimeters, with each clamp registering a mass of 133.17 grams.



Figure 1: Selected CAD model

Subsequently, a Static Test was conducted within the Simulation Module of Fusion 360 software to assess the structural integrity of the component when subjected to a 50 N load. The parameters governing this evaluation are delineated in Table 3 and are visually represented in Figure 2. This assessment is the preliminary phase for the ensuing Additive Manufacturing (AM) optimization process, facilitated using nTopology software. The primary objective of this optimization is to achieve mass reduction while preserving the component's ability to support objects with a minimum weight capacity of 5 kilograms, all while maintaining a minimum safety factor of 3. It is pertinent to note that the selection of an appropriate safety factor necessitates careful consideration of multiple factors, encompassing the material properties, final cost, operating conditions, design attributes, analytical rigor, and manufacturing processes (Mascarenhas, Ahrens and Ogliari 2004). In this specific context, a safety factor of 3 has been deemed adequate to affirm the structural soundness of the component.

Material	AISI 316L stainless steel
Constraints	Fix holes for the axis.
Load Case	50 N applied on the Gripper Clamp contact zone Gravity Force

Table 3: Typical mechanical properties for 316L (Granta CES EDUPACK, 2022)

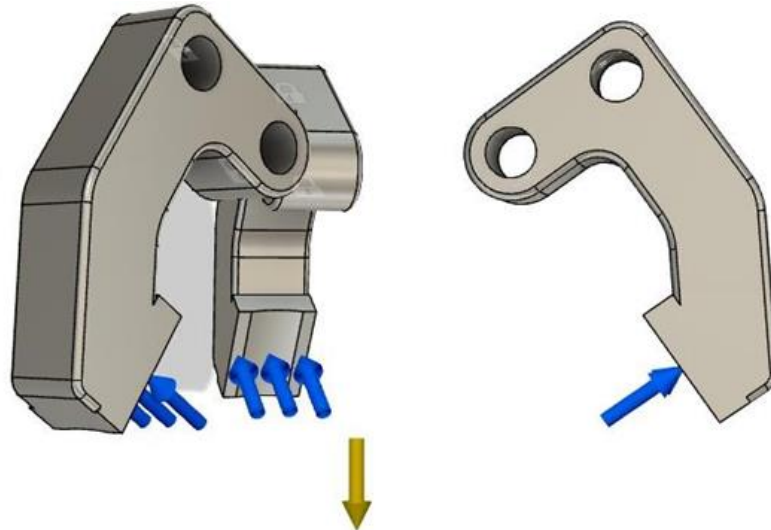


Figure 2: Load cases and constraints used on static stress simulation, forces applied on the contact zone of the gripper clamp are marked with the blue arrows and the gravitational force is marked with the gold arrow.

Following this, the topology optimization of the Gripper Clamps was executed employing the nTopology software. Two different topology optimizations were performed since, as discussed in the next chapter, the first topology optimization did not achieve the defined goals. To initiate this endeavor, the requisite steps encompassed the creation of a Finite Element (FE) model, the establishment of an FE volume mesh, material definition, imposition of Boundary Conditions, and the formulation of a Topology Optimization block that aimed to minimize mass. In the selection of material, AISI 316L stainless steel was chosen owing to its commendable mechanical properties, as previously discussed. Detailed parameters and a graphical representation of this optimization process are delineated in [Figure 3](#) and comprehensively summarized in [Table 4](#).

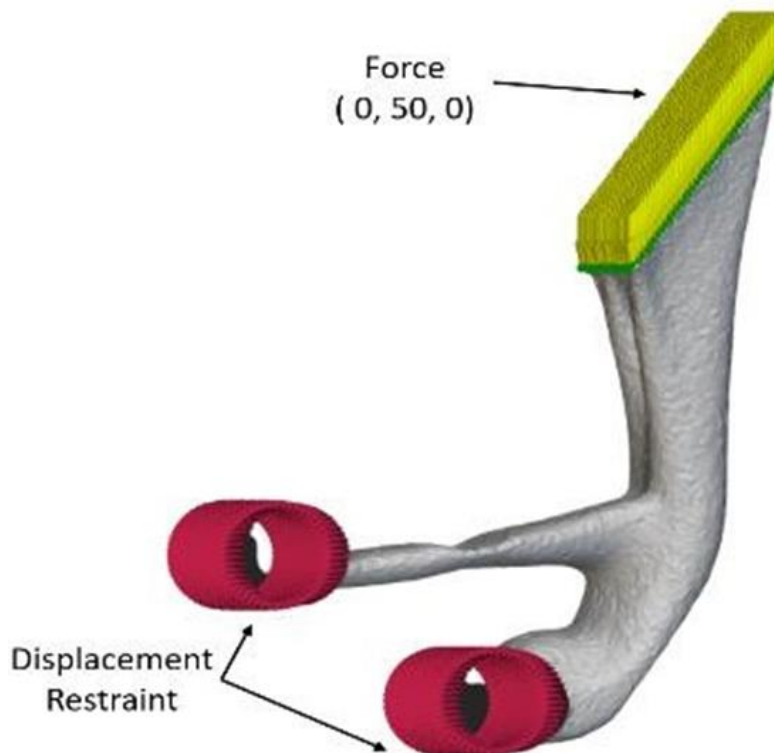


Figure 3: Boundary conditions used.

Component Name	A	B
Material	AISI 316L stainless steel	
Volume Fraction Constraint	0.3	0.4
Iteration	57	47
Force	(0, 50, 0) N	

Table 4: Parameters used in topology optimizations.

2.3. Lightweighting

Applying weight reduction strategies through the incorporation of periodic lattice structures was considered a judicious approach to diminish the component's mass while preserving its mechanical attributes. This approach was particularly pertinent given the substantial heft of the clamp support, which approximated 3138.43 kilograms. In this pursuit, as illustrated in Figure 4, two distinct lattice configurations were employed: the SlitP lattices (denoted as 1 and 4) and the Gyroid lattices (referred to as 2 and 3).

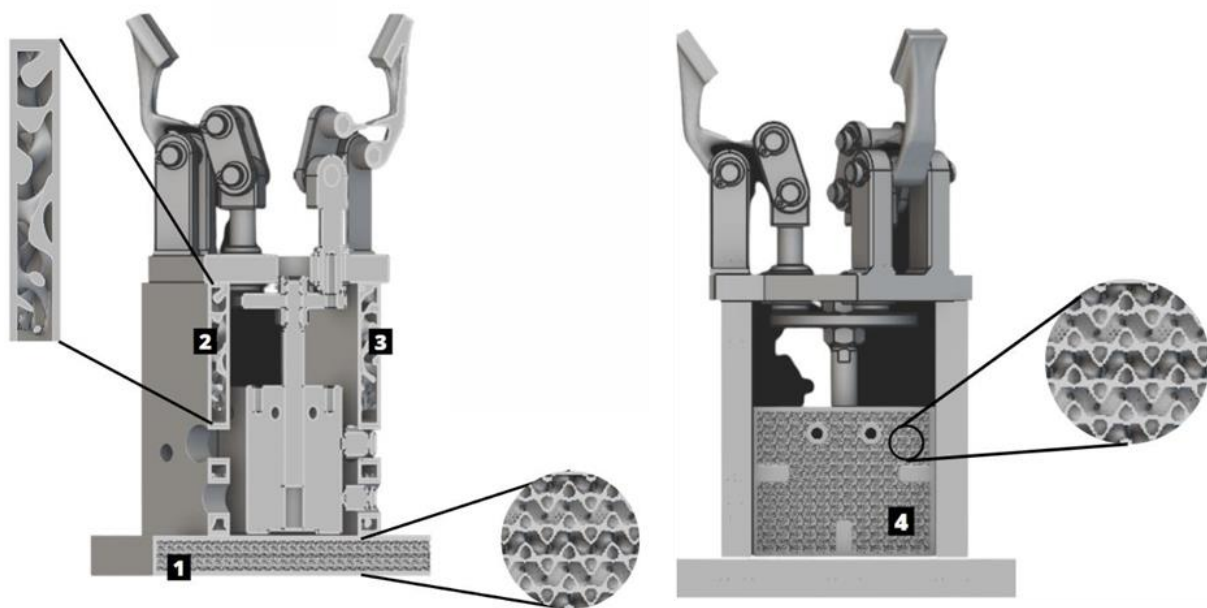


Figure 4: Lightweighting operations, where 1 and 4 use SplitP lattices and 2 and 3 Gyroid lattices.

2.4. Simulation

The simulations were executed using Fusion 360, and the specific parameters employed are comprehensively documented in Table 3, except for the varied load cases. Throughout these simulations, the conditioned faces pertained to the holes designated for shaft insertion, and the load cases, distinguished by their blue highlighting within the contact area of the gripper clamp, were explicitly defined. Of particular significance, the load case highlighted by the gold arrow represents the constant gravitational force, maintained as a consistent factor across all simulation runs, as depicted in Figure 2. The first simulation was performed on the clamps originated by topology optimization A, with an applied load case of 50 N. The following static stress simulations were run on component B using the same settings as those in component A, but with different load scenarios.

3. Discussion

Table 5 displays the outcomes of the simulation of the original CAD file's gripper clamps, which have an initial weight of 399.503 g.

Safety Factor	Displacement	Yield Strength
15	0.0020mm	4.506 MPa

Table 5: Results obtained in the simulation of the original CAD file’s gripper clamps.

The findings underscore an over-dimensioning of the Gripper Clamp, characterized by a notable minimum safety factor of 15. Subsequently, two distinct topology optimization procedures were undertaken, as detailed in the preceding section. Their outcomes, along with the results obtained from the static stress simulation conducted under a 50 N load, are meticulously delineated in [Table 6](#).



Topology Optimization	A	B
Model		
Mass(g)	167.00	200.98
Mass Deduction	57.95%	49.72%
Min. Safety Factor	1.32	15
Max. Yield Strength (MPa)	126.7	56.7
Max. Displacement (mm)	0.040	0.027

Table 6: Results obtained in the topology optimization A and B, and the respective simulation results when a load of 50 N was applied.

Studying the simulation results of topology optimization A, it became evident that this particular component needed to offer a practical solution. While intriguing in its concept, the pursuit of further development in this direction was deemed unfeasible. Consequently, the decision was made to discontinue the model's exploration to conserve time, leading to the omission of additional simulation iterations. It should be emphasized that no plastic deformation took place since the greatest stress the material can endure, roughly 170 MPa, is higher than the maximum stress obtained in this test. However, the goal remains to withstand a load of at least 5 kg while ensuring a safety factor 3. Thus, it was necessary to increase the mechanical properties without increasing the mass exceedingly. Therefore, component B was obtained, changing the volume fraction constraint from 0.3 to 0.4 and adapting the model to improve the safety factor. Upon closely examining the data pertaining to component B, it becomes apparent that a mere increase of 32.99 grams yielded a substantial augmentation in the safety factor while concurrently effecting a significant reduction in mass, which escalated to 49.72%.

Across several simulations on Fusion 360, it was determined that the maximum load case that these clamps from Model could sustain the maximum load, with a safety factor of 3, without incurring deformation, up to approximately 12 kilograms, as shown in [Table 7](#) and [Figure 5](#). Applying this load, this component exhibits no significant displacement or deformation, as 56.7 MPa is a lower value than the yield strength of 316L Stainless Steel.

Load Case	Safety Factor	Displacement	Yield Strength
120 N	3	0.040 mm	56.7 MPa

Table 7: Results obtained in the simulation of topology optimization B when a load case of 120 N was applied.

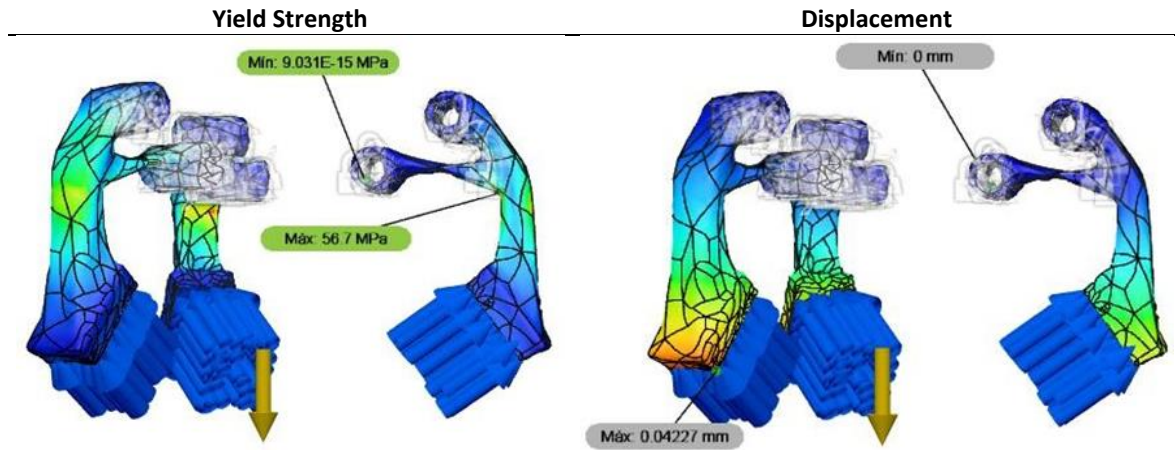


Figure 5: Test simulation results for the displacement and yield strength obtained for component B, when applied a load case of 120 N.

Regarding lightweight operations, the results found are presented in Table 8. The components are numbered according to Figure 4 in the previous chapter.

Load Case	Safety Factor	Displacement	Yield Strength
120 N	3	0.040 mm	56.7 MPa

Table 8: Results obtained in the simulation of topology optimization B when a load case of 120 N was applied.

Analyzing Table 8, it can be detected that a significant mass reduction, above 35%, has been achieved with the lightweight operations. Due to the complexity of the file, it was not possible to evaluate the impact of these deviations in the mechanical resistance of the gripper clamp in its integrity. However, when conducting these operations, holes for the screws and a thickness of 3 mm in all the components' walls were considered, ensuring structural stability. With component B identified as the definitive outcome of the topology optimization process for the gripper clamps, coupled with the incorporation of the weight reduction measures, a total reduction of 26.30% in the weight of the clamps was successfully achieved.

4. Conclusions

The primary objective of this study was to undertake the design and optimization of a gripper clamp, employing nTopology and Fusion 360 software, with the aim of enabling its potential production via additive manufacturing. The application of nTopology software afforded a degree of flexibility in terms of topology optimization and facilitated the utilization of lattice structures for weight reduction. To carry out this work, it was necessary to convert the nTopology file to an STL file so that it was possible to use Fusion 360 software. However, this conversion resulted in some loss of critical information that could have influenced the simulation outcomes. Since the file was very complex, it was impossible to simulate the gripper in Fusion 360 fully.

The initial topology optimization with a fractional volume constraint set at 0.3, referred to as component A, yielded results that failed to align with the predefined criteria and were consequently dismissed. Subsequent topology optimization with a fractional volume constraint of 0.4, identified as component B, demonstrated positive outcomes. It showcased a significant mass reduction of 49.72%. It proved capable of withstanding a load of up to 12 kilograms while maintaining a safety factor of 3, all the while exhibiting negligible displacement and incorporating light-weighting measures, including the introduction of SlitP and Gyroid-type lattice structures, a substantial foundation weight reduction exceeding 35% was achieved. Viewing component B as the ultimate topology optimization for the claws and

accounting for the weight reduction procedures, an overall reduction of 26.30% in the mass of the gripper claw was successfully realized. This evaluation considered the mechanical properties of the final component.

In conclusion, despite the inherent challenges, the optimization modeling phase yielded dependable and promising outcomes. Concurrently, the chosen material was validated as a suitable and proficient solution for the intended application.

5. Future works

The prospect of conducting a comprehensive simulation of the entire model as a cohesive unit is of considerable interest. Regrettably, this endeavor proved unfeasible primarily due to the formidable size of the file. In further research, an avenue worth exploring involves extending the present study to encompass alternative materials, such as composite polymers reinforced with carbon fiber, a domain suitable for employment with the FFF process, or potentially an aluminum alloy, which aligns with the LPBF technology.

References

- “9450P PLATEABLE GRADE.” 1990. Alloy Digest 39 (11): P-20. <https://doi.org/10.31399/asm.ad.p0020>.
- Bedmar, J., S. García-Rodríguez, M. Roldán, B. Torres, and J. Rams. 2022. “Effects of the Heat Treatment on the Microstructure and Corrosion Behavior of 316 L Stainless Steel Manufactured by Laser Powder Bed Fusion.” Corrosion Science 209 (December): 110777. <https://doi.org/10.1016/j.corsci.2022.110777>.
- Costa, José, Elsa Sequeiros, Maria Teresa Vieira, and Manuel Vieira. 2021. “Additive Manufacturing: Material Extrusion of Metallic Parts.” U.Porto Journal of Engineering 7 (3): 53–69. https://doi.org/10.24840/2183-6493_007.003_0005.
- Criales, Luis E., Yiğit M. Arisoy, Brandon Lane, Shawn Moylan, Alkan Donmez, and Tuğrul Özel. 2017. “Laser Powder Bed Fusion of Nickel Alloy 625: Experimental Investigations of Effects of Process Parameters on Melt Pool Size and Shape with Spatter Analysis.” International Journal of Machine Tools and Manufacture 121 (October): 22–36. <https://doi.org/10.1016/j.ijmactools.2017.03.004>.
- DebRoy, T., H.L. Wei, J.S. Zuback, T. Mukherjee, J.W. Elmer, J.O. Milewski, A.M. Beese, A. Wilson-Heid, A. De, and W. Zhang. 2018. “Additive Manufacturing of Metallic Components – Process, Structure and Properties.” Progress in Materials Science 92 (March): 112–224. <https://doi.org/10.1016/j.pmatsci.2017.10.001>.
- Diaz Vallejo, Nathalia, Cameron Lucas, Nicolas Ayers, Kevin Graydon, Holden Hyer, and Yongho Sohn. 2021. “Process Optimization and Microstructure Analysis to Understand Laser Powder Bed Fusion of 316L Stainless Steel.” Metals 11 (5): 832. <https://doi.org/10.3390/met11050832>.
- Ford, Simon, and Mélanie Despeisse. 2016. “Additive Manufacturing and Sustainability: An Exploratory Study of the Advantages and Challenges.” Journal of Cleaner Production 137 (November): 1573–87. <https://doi.org/10.1016/j.jclepro.2016.04.150>.
- Gibson, Ian, David W. Rosen, and Brent Stucker. 2010. Additive Manufacturing Technologies: Rapid Prototyping to Direct Digital Manufacturing. Boston, MA: Springer US. <https://doi.org/10.1007/978-1-4419-1120-9>.
- Gorsse, Stéphane, Christopher Hutchinson, Mohamed Gouné, and Rajarshi Banerjee. 2017. “Additive Manufacturing of Metals: A Brief Review of the Characteristic Microstructures

- and Properties of Steels, Ti-6Al-4V and High-Entropy Alloys.” *Science and Technology of Advanced Materials* 18 (1): 584–610. <https://doi.org/10.1080/14686996.2017.1361305>.
- Herderick, E. 2011. “Additive Manufacturing of Metals: A Review.” In *Proceedings of MS&T’11*. Columbus, OH. <https://www.semanticscholar.org/paper/Additive-Manufacturing-of-Metals%3A-A-Review-Herderick/156b0bcef5d03cdf0a35947030c1c0729ca923d3>.
- Huang, Yong, Ming C. Leu, Jyoti Mazumder, and Alkan Donmez. 2015. “Additive Manufacturing: Current State, Future Potential, Gaps and Needs, and Recommendations.” *Journal of Manufacturing Science and Engineering* 137 (1): 014001. <https://doi.org/10.1115/1.4028725>.
- Irrinki, Harish, Subrata D. Nath, Arulselvan Arumugham Akilan, and Sundar V. Atre. 2020. “Laser Powder Bed Fusion.” In *Additive Manufacturing Processes*, edited by David L. Bourell, William Frazier, Howard Kuhn, and Mohsen Seifi, 209–19. ASM International. <https://doi.org/10.31399/asm.hb.v24.a0006621>.
- ISO/ASTM. 2015. “ISO/ASTM 52900:2015(E) Additive manufacturing — General principles — Terminology.” Accessed February 1, 2024. <https://www.iso.org/standard/69669.html>.
- Khairallah, Saad A., Andrew T. Anderson, Alexander Rubenchik, and Wayne E. King. 2016. “Laser Powder-Bed Fusion Additive Manufacturing: Physics of Complex Melt Flow and Formation Mechanisms of Pores, Spatter, and Denudation Zones.” *Acta Materialia* 108 (April): 36–45. <https://doi.org/10.1016/j.actamat.2016.02.014>.
- King, W. E., A. T. Anderson, R. M. Ferencz, N. E. Hodge, C. Kamath, S. A. Khairallah, and A. M. Rubenchik. 2015. “Laser Powder Bed Fusion Additive Manufacturing of Metals; Physics, Computational, and Materials Challenges.” *Applied Physics Reviews* 2 (4): 041304. <https://doi.org/10.1063/1.4937809>.
- Mascarenhas, W.N., C.H. Ahrens, and A. Ogliari. 2004. “Design Criteria and Safety Factors for Plastic Components Design.” *Materials & Design* 25 (3): 257–61. <https://doi.org/10.1016/j.matdes.2003.10.003>.
- Mata, Margarida, Mateus Pinto, and José Costa. 2023. “Topological Optimization of a Metal Extruded Doorhandle Using nTopology.” *U.Porto Journal of Engineering* 9 (1): 42–54. https://doi.org/10.24840/2183-6493_009-001_001620.
- Oliveira, Carolina, Mariana Maia, and José Costa. 2023. “Production of an Office Stapler by Material Extrusion Process, Using DfAM as Optimization Strategy.” *U.Porto Journal of Engineering* 9 (1): 28–41. https://doi.org/10.24840/2183-6493_009-001_001635.
- Rosinha, Inês P., Krist V. Gernaey, John M. Woodley, and Ulrich Krühne. 2015. “Topology Optimization for Biocatalytic Microreactor Configurations.” In *Computer Aided Chemical Engineering*, 37:1463–68. Elsevier. <https://doi.org/10.1016/B978-0-444-63577-8.50089-9>.
- Tang, X. 2005. “Sigma Phase Characterization in AISI 316 Stainless Steel.” *Microscopy and Microanalysis* 11 (S02). <https://doi.org/10.1017/S143192760550374X>.
- Tofail, Syed A.M., Elias P. Koumoulos, Amit Bandyopadhyay, Susmita Bose, Lisa O’Donoghue, and Costas Charitidis. 2018. “Additive Manufacturing: Scientific and Technological Challenges, Market Uptake and Opportunities.” *Materials Today* 21 (1): 22–37. <https://doi.org/10.1016/j.mattod.2017.07.001>.
- Vander Voort, George F., ed. 2004. *Metallography and Microstructures*. ASM International. <https://doi.org/10.31399/asm.hb.v09.9781627081771>.

Zitelli, Folgarait, and Di Schino. 2019. "Laser Powder Bed Fusion of Stainless Steel Grades: A Review." *Metals* 9 (7): 731. <https://doi.org/10.3390/met9070731>.